

Photodegradation of Methylene Blue by LaFeO₃/ZnO Nanocomposites under Visible and UV Light Irradiation

Nur Afifah^{1,2} and Rosari Saleh^{1,2,a}

¹Departemen Fisika, Fakultas MIPA, Universitas Indonesia, Kampus UI Depok, 16424 Depok, Indonesia

²Integrated Laboratory of Energy and Environment, Fakultas MIPA, Universitas Indonesia, Kampus UI Depok, 16424 Depok, Indonesia

^aCorresponding's author: rosari.saleh@gmail.com, rosari.saleh@ui.ac.id

Abstract. In this study, LaFeO₃/ZnO nanocomposites with different molar ratios of ZnO (0.1, 0.3, 0.5, and 1) have been prepared using the sol-gel method. The structural and elemental analyses of the samples were measured by X-ray diffraction (XRD) and X-ray fluorescence (XRF) spectroscopy. XRD results showed that the synthesized samples exhibited an orthorhombic structure of LaFeO₃ and a hexagonal wurtzite structure of ZnO. However, the ZnO hexagonal wurtzite structure could not be detected below the ZnO molar ratio of 0.5. The presence of ZnO on the nanocomposites was confirmed using XRF measurements. The results revealed that the XRF spectra of the samples consisted of La, Fe, and Zn atoms. The photodegradation of methylene blue (MB) using LaFeO₃/ZnO nanocomposites was then monitored under visible and UV light irradiation. The photodegradation results showed that the presence of LaFeO₃/ZnO nanocomposites could degrade the MB solution. The highest MB degradation was found in the presence of ZnO at a molar ratio of 0.5. All of the LaFeO₃/ZnO nanocomposites showed better photocatalytic performance than did LaFeO₃ nanoparticles alone. Furthermore, several parameters, such as the effect of catalyst dose, initial concentration of MB, and various radical scavengers, were also measured to obtain the maximum condition and the main active species involved in the photocatalytic process.

1. Introduction

Photocatalysis is the process of destroying the complex chemical bonds of organic or inorganic pollutants to transform them into harmless chemicals using a photocatalyst and light as an irradiation source [1]. Among several photocatalysts, ZnO has shown great potential due to its high catalytic activity, high electron mobility, high photosensitivity, chemical stability, low price and non-toxicity [2-4]. However, ZnO has a low response in the visible light region, and high electron and hole-pair recombinations due to its wide band gap of about 3.2 eV and low quantum efficiency, which hinders its use in practical applications [5-6]. However, coupling ZnO with narrow band gap catalysts is a promising solution to this problem by extending the photoresponse of ZnO into the visible light region and maximizing the utilization of sunlight as a renewable energy source [7].

A catalyst that has been widely used in the visible light region is perovskite, LaFeO₃. LaFeO₃ has attracted considerable attention due to its structural stability, suitable gaps in the visible light region, and unique optoelectronic properties [8-9]. Perovskite materials as catalysts also show high efficiency, high thermal stability, nontoxicity, and unique physicochemical properties [10]. The photocatalytic activity of perovskite materials such as LaFeO₃ [11] and LaMnO₃ [12] nanoparticles has been reported in our previous work. However, its photocatalytic performance didn't showed the complete degradation

of MB solution due to its high electron and hole recombination. In order to fully utilize sunlight, LaFeO₃ can be combined with ZnO to improve its photocatalytic performance by inhibiting the electron and holes recombination. Moreover, combining LaFeO₃ as visible light catalyst and ZnO as UV light catalyst in this study is expected to extend the catalyst response in both visible and UV light irradiation. The LaFeO₃/ZnO nanocomposites can also be applied as the promising catalyst in the sunlight as a renewable energy source. Furthermore, several parameters that play important roles in the photocatalytic process were studied and discussed.

2. Experimental details

Catalyst preparation: LaCl₃•7H₂O, FeCl₂•4H₂O, ZnSO₄•7H₂O, and NaOH were purchased from Merck to be used as raw materials without further purification. The LaFeO₃/ZnO nanocomposites with different molar ratios of ZnO (0.1, 0.3, 0.5, and 1) were obtained by the sol-gel method. Briefly, solution A was prepared by dissolving 0.00125 mol ZnSO₄•7H₂O into 31 ml of distilled water under a magnetic stirrer. Then, 0.0025 NaOH was added to 62 ml of distilled water and dissolved into solution A until a pH value of 12 was reached. After that, the mixture was stirred and heated to a temperature of 80 °C. Meanwhile, solution B was obtained by dissolving the LaFeO₃ nanoparticles (prepared by following our previous work [11]) into 31 ml of distilled water. Solution B was then dissolved into solution A under the continuous agitation of the magnetic stirrer at 80 °C for 2 hours. Simple centrifugation was used to separate the precipitate and the solution. Finally, the precipitate was allowed to stand overnight at room temperature, then dried at 120 °C for one hour under vacuum conditions.

Characterization: The LaFeO₃/ZnO nanocomposite crystal structures were characterized by X-ray diffraction (XRD) measurements. A monochromatic Cu-K_α ($\lambda = 1.54060 \text{ \AA}$), which operated at 30 kV and 20 mA in the range of 10°–90°, was used as the radiation source. The elemental analyses of the samples and the concentration (C) of each element were analyzed using X-ray fluorescence (XRF) spectroscopy.

Photocatalytic experiment: The photodegradation of MB in the presence of LaFeO₃/ZnO nanocomposites as catalysts was performed under visible and UV light irradiation. First, an amount of catalyst was added to MB solution under a magnetic stirrer. Then, the solution was then kept in dark for 30 min to reach absorption and desorption equilibrium. After that, the solution was treated under light irradiation using a 40W Xe lamp or a 40W UV lamp as the visible and UV light sources, respectively. Finally, to obtain the percentage degraded MB, the 10 ml of MB solution was collected at different time intervals and then analyzed using a UV-visible spectrophotometer. In order to obtain the maximum condition in the photocatalytic experiment, the effects of catalyst dosage and initial concentrations of MB were investigated. Moreover, the effects of various radical scavengers were also determined to obtain the main active species involved in the photocatalytic process. Sodium sulfate, di-ammonium oxalate, and tert-butyl alcohol were used as electrons, holes, and hydroxyl radical scavengers, respectively.

3. Results and Discussion

The XRD pattern of the ZnO nanoparticles, LaFeO₃ nanoparticles, and LaFeO₃/ZnO nanocomposites with different molar ratios of ZnO are shown in Figure 1a. The XRD lines of the ZnO nanoparticles were observed at 31.73° (100), 34.35° (002), 36.22° (101), 47.52° (102), 56.51° (110), 62.82° (103), 66.42° (200), 67.89° (112), and 69.04° (201), which are well indexed by the hexagonal wurtzite structure of ZnO [13-14]. Meanwhile, the XRD lines of LaFeO₃ nanoparticles were observed at 22.6° (101), 32.2° (121), 39.8° (220), 46.2° (202), 57.5° (240), 67.4° (242), and 76.7° (204), which are well indexed by the orthorhombic structure of LaFeO₃ [15-16]. Moreover, all diffraction peaks of LaFeO₃/ZnO nanocomposites were in agreement with those of the standard patterns for orthorhombic LaFeO₃ and hexagonal wurtzite ZnO. However, at the low ZnO molar ratio, the hexagonal wurtzite structure of ZnO could not be detected, possibly due to the lower ZnO content in the nanocomposites. The grain size $\langle D \rangle$ of the prepared samples was calculated using the Debye-Scherrer equation [17]: $\langle D \rangle = 0.9\lambda/\beta\cos\theta$, where λ is the Cu-K_α wavelength, β is the full width of half-maximum, and θ is the Bragg angle. The

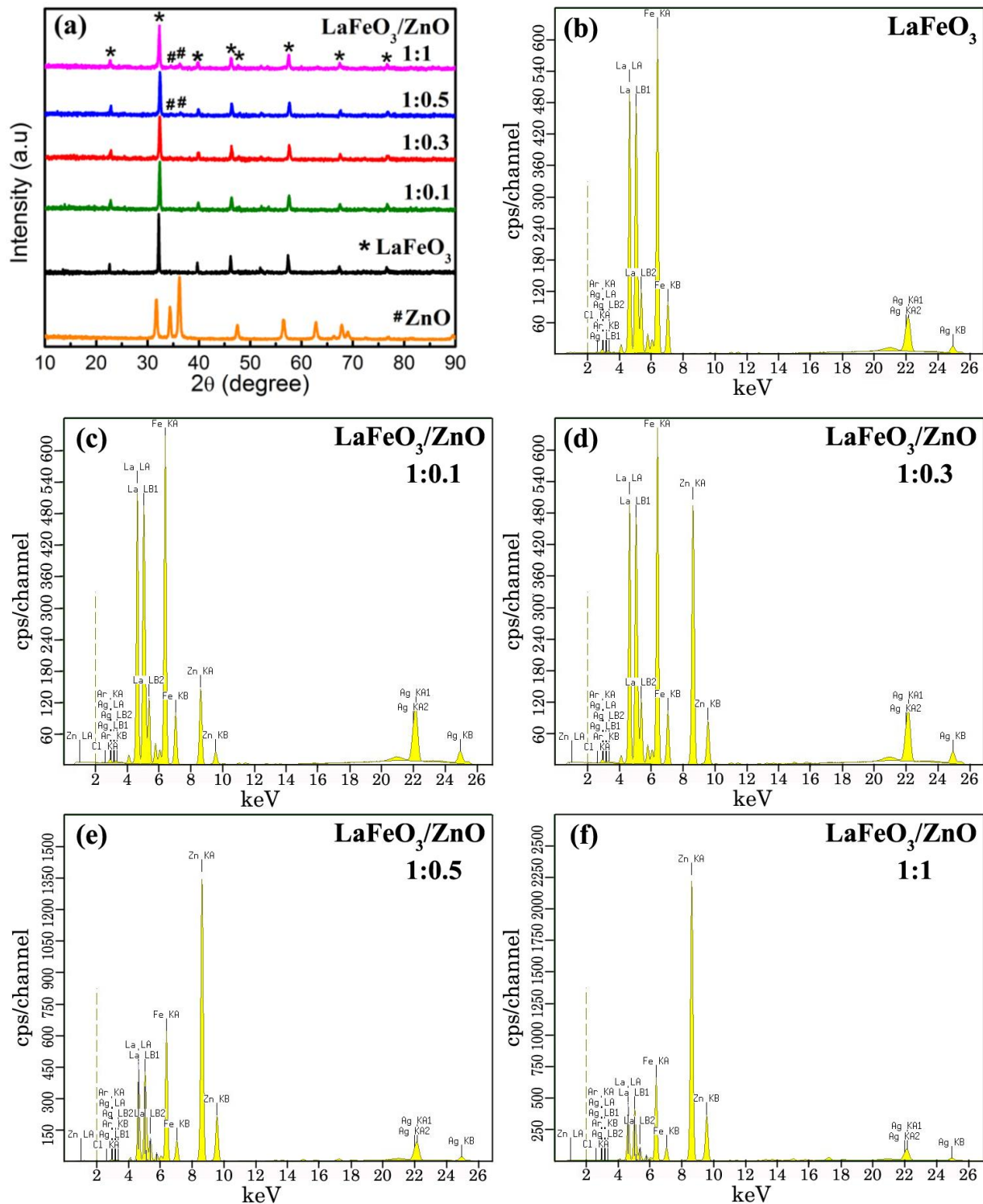


Figure 1. (a) XRD pattern; and (b-f) XRF spectra of $\text{LaFeO}_3/\text{ZnO}$ nanocomposites with different molar ratios of ZnO.

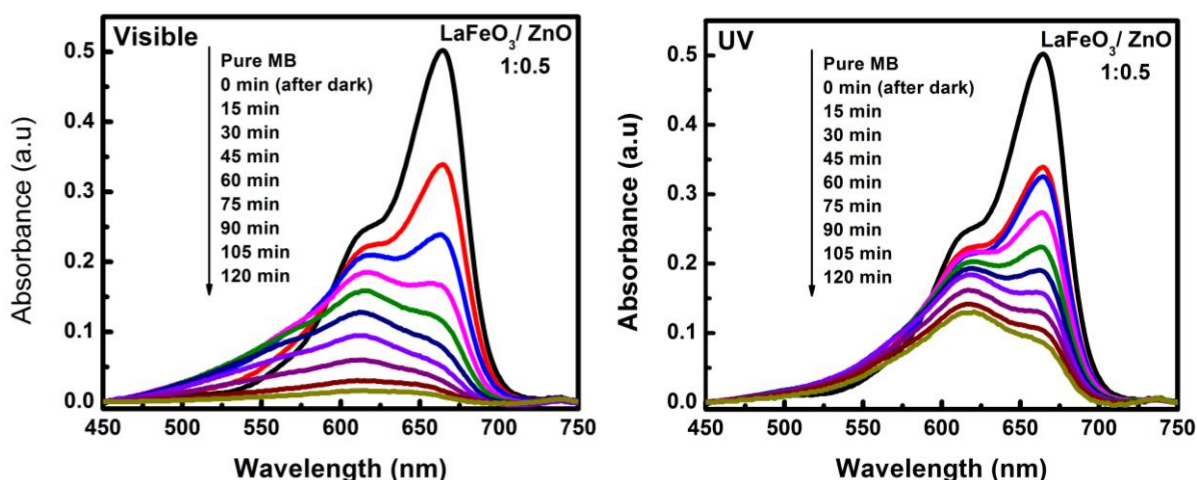
(121) peak of LaFeO_3 and (101) peak of ZnO were used to estimate the crystallite size, and the values are tabulated in Table 1. The lattice parameter calculated by the Rietveld refinement method using the MAUD program is also tabulated in Table 1.

Table 1. The lattice parameter and grain size $\langle D \rangle$ of $\text{LaFeO}_3/\text{ZnO}$ nanocomposites.

Sample	Molar Ratio	Lattice Parameter LaFeO_3			Lattice Parameter ZnO		$\langle D \rangle$ LaFeO_3	$\langle D \rangle$ ZnO
		a (Å)	b (Å)	c (Å)	a=b (Å)	c (Å)	(nm)	(nm)
$\text{LaFeO}_3/\text{ZnO}$	1:0	5.5436	7.8456	5.5528	-	-	58	-
	1:0.1	5.5205	7.8263	5.5503	3.2088	5.2368	37	30
	1:0.3	5.5948	7.8771	5.5640	3.2180	5.2344	31	26
	1:0.5	5.4970	7.8220	5.5492	3.2305	5.2484	28	24
	1.1	5.5402	7.8407	5.5537	3.2356	5.2497	25	21

Table 2. The chemical composition of $\text{LaFeO}_3/\text{ZnO}$ nanocomposites.

Sample	Molar Ratio	La	Fe	Zn	Cl
		Concentration (%)	Concentration (%)	Concentration (%)	Concentration (%)
$\text{LaFeO}_3/\text{ZnO}$	1:0	71.621	26.834	0	1.545
	1:0.1	71.186	26.184	2.436	0.195
	1:0.3	66.395	25.451	7.923	0.232
	1:0.5	57.714	21.653	20.435	0.198
	1.1	52.040	20.045	27.759	0.156

**Figure 2.** The UV-Visible spectra of MB solution at different time intervals.

The elemental analyses of the prepared samples were performed using XRF spectroscopy. Figure 1(b-f) shows the XRF spectra of the $\text{LaFeO}_3/\text{ZnO}$ nanocomposites with different molar ratios of ZnO . As a comparison, the XRF spectra of the LaFeO_3 nanoparticles are also shown. The XRF spectra of the LaFeO_3 nanoparticles and $\text{LaFeO}_3/\text{ZnO}$ nanocomposites consisted of La and Fe atoms, while the Zn peak was also detected in the XRF spectra of the nanocomposites. The presence of Zn atoms in the samples confirmed the formation of $\text{LaFeO}_3/\text{ZnO}$ in the nanocomposite form. The appearance of Ag, Ar, and Cl peaks in the spectra were confirmed by the X-ray tube anode element of the XRF tools. The chemical composition of each element was also determined by XRF measurements. The concentration (C) of each element is tabulated in Table 2. As seen in the table, the concentration of elemental Zn increased with the increasing ZnO molar ratio.

To evaluate the photocatalytic activity of the prepared sample, MB degradation was monitored. During the visible and UV light irradiation in the presence of $\text{LaFeO}_3/\text{ZnO}$ nanocomposites as catalysts,

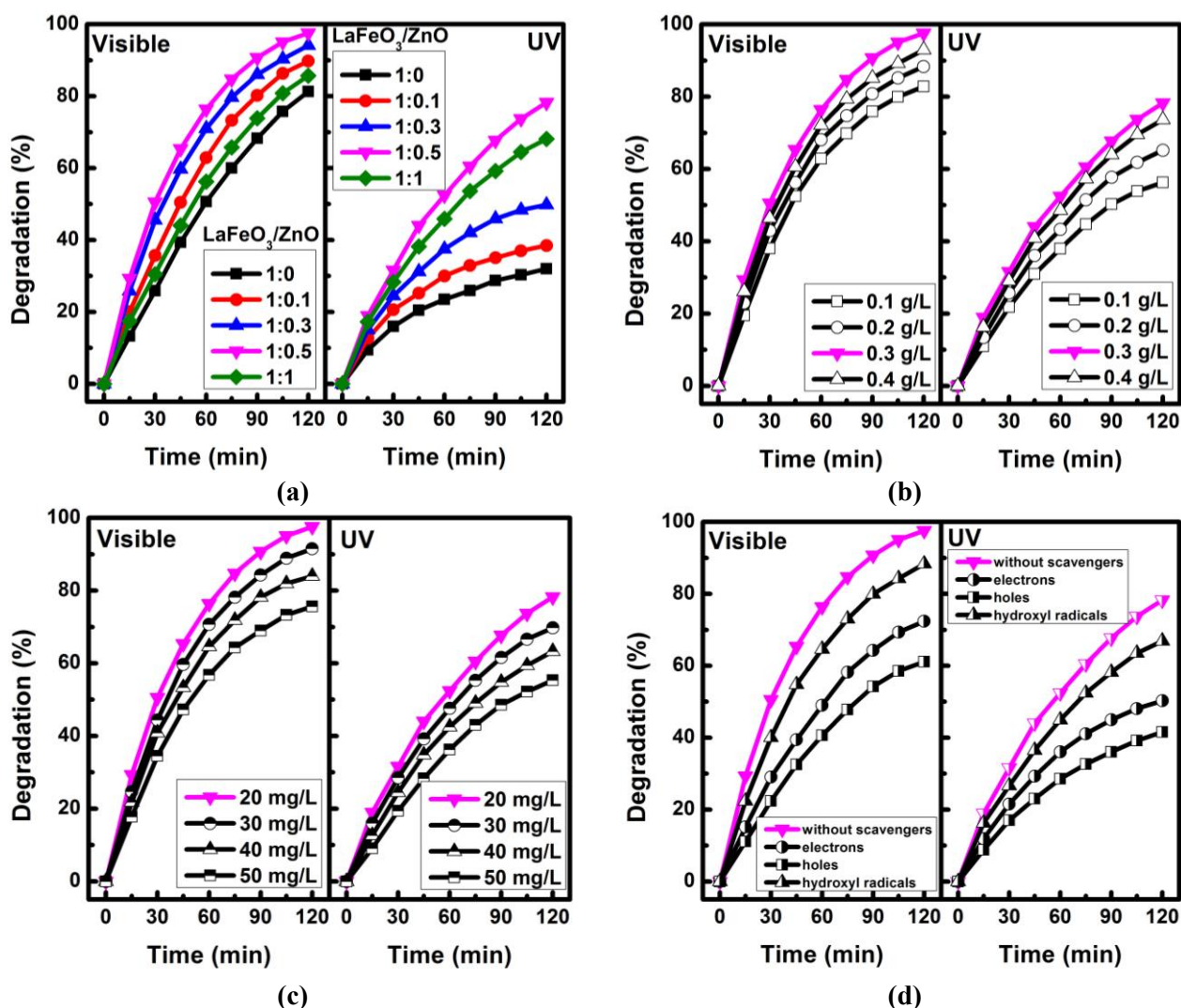


Figure 3. The percentage of degraded MB in the presence of different LaFeO₃/ZnO molar ratios (a). The effect of catalyst dosage (b), initial concentration of MB (c), and various radical scavengers (c) on the percentage of degraded MB.

the MB color gradually changed to colorless, which was further confirmed by monitoring the UV-visible spectra (450–750 nm) of the MB solution at different time intervals, as shown in Figure 2. The UV-visible absorbance spectra was then used to study the photocatalytic efficiency in terms of percentage of degraded MB with the following equation [17]: $\text{Degradation (\%)} = ((C_0 - C_t)/C_0) \times 100$, where C_0 is the MB initial concentration (after dark) and C_t is the MB concentration at each irradiated time interval (min). The percentage of degraded MB under visible and UV light irradiation in the presence of different LaFeO₃/ZnO molar ratios is shown in Figure 3a. The percentage of degraded MB in the presence of LaFeO₃ nanoparticles is also shown as a comparison. The obtained results revealed that the incorporation of ZnO in the nanocomposite form could increase the degradation efficiency of LaFeO₃ nanoparticles. The incorporation of ZnO into the nanocomposite could serve as an electron trapper, which would inhibit electron and hole recombinations and enhance the photocatalytic performance [13, 18]. The LaFeO₃/ZnO nanocomposites at a molar ratio of 1:0.5 showed the best degradation efficiency both under visible and UV light irradiation.

To obtain the maximum condition, several parameters were adjusted in the photocatalytic experiments. Figure 3b shows the effect of catalyst dosage on the percentage of degraded MB using

LaFeO₃/ZnO nanocomposites at a molar ratio of 1:0.5 under visible and UV light irradiation. The initial MB concentration was held constant at 20 mg/L. As seen in the figure, the degradation efficiency increased with the increasing catalyst dosage from 0.1 g/L to 0.3 g/L; thereafter, at the catalyst dosage of 0.4 g/L, the degradation efficiency decreased. At lower maximum catalyst dosages, low active sites were available, while at higher maximum catalyst dosages, agglomerated particles, high turbidity, and scattering effects might cause lower degradation efficiency [13, 19]. Furthermore, the effects of MB initial concentration on the photocatalytic performance of LaFeO₃/ZnO nanocomposites were also evaluated under visible and UV light irradiation. The LaFeO₃/ZnO nanocomposites at a molar ratio of 1:0.5 and the catalyst with maximum dosage concentration of 0.3 g/L were used as the dependent parameters, while the initial concentration of MB varied from 20 mg/L to 50 mg/L. The results presented in Figure 3c show that the lower initial concentration of MB exhibited the best photocatalytic performance. At higher initial concentrations of MB, the penetration of light that could travel to the active site of the catalyst was blocked, resulting in a decrease in the total number of active sites that played roles in the degradation process [20].

It has been reported that photocatalytic activity depends on the number of active species that play important roles in the photocatalytic process [18, 21]. During irradiation, excited electrons in the conduction band of the catalyst react with the oxygen molecules (O₂) to form superoxide radicals (•O₂). In contrast, holes left behind in the valence band of the catalyst will react with water (H₂O) or hydroxyl (OH⁻) molecules to form hydroxyl radicals (•OH). These active radicals are known as strong reducers and oxidizers, which can destroy the complex chemical bonds of dyes such as MB [21]. For this reason, a control experiment with the addition of a scavenger such as electrons, holes, and hydroxyl radicals would be interesting to monitor. Sodium sulfate, di-ammonium oxalate, and tert-butyl alcohol were used as electrons, holes, and hydroxyl radical scavengers, respectively, in this study. After a 2-hour irradiation time, the presence of hydroxyl radical scavengers (as shown in Figure 3d) decreased the degradation of LaFeO₃/ZnO nanocomposites without additional scavengers. Moreover, the presence of electron scavengers further decreased the degradation efficiency. The lowest degradation was obtained in the presence of di-ammonium oxalate as a hole scavenger, indicating that holes are the main active species in the photodegradation of MB.

4. Conclusion

The photodegradation of MB using LaFeO₃/ZnO nanocomposites with different molar ratios of ZnO was successfully monitored under visible and UV light irradiation. The presence of ZnO in the orthorhombic and hexagonal wurtzite structures of the LaFeO₃/ZnO nanocomposites improved the photocatalytic performance of the LaFeO₃ nanoparticles. The concentration of 0.3 g/L of LaFeO₃/ZnO nanocomposite at a molar ratio of 1:0.5 exhibited the best photocatalytic performance for degrading a 20 mg/L MB solution. The main active species in the photocatalytic process is holes followed by electrons and hydroxyl radical scavengers.

References

- [1] Sakellis I, Giamini S, Moschos I, Chandrinou C, Travlos , Kim C-Y, Lee J-H, Kim J-G and Boukos N 2014 *Energ. Procedia* **60** 37
- [2] Mekasuwandumrong O, Pawinrat P, Praserttham P and Panpranot J 2010 *Chem. Eng. J.* **164** 77
- [3] Xia Y, Zhang W, Zhang Y, Yu X and Chen F 2014 *Mater. Lett.* **131** 178
- [4] Fu X, Xie M, Luan P and Jing L 2014 *ACS Appl. Mater. Interfaces* **6** 18550
- [5] Guo X, Zhu H and Li Q 2014 *Appl. Catal. B.* **160–161** 408
- [6] Awasthi G P, Adhikari S P, Ko S, Kim H J, Park C H and Kim C S 2016 *J. Alloy. Compd.* **682** 208
- [7] He Z, Xia Y, Tang B, Jiang X and Su J 2016 *Mater. Lett.* **184** 148
- [8] Shen H, Xue T, Wang Y, Cao G, Lu Y and Fang G 2016 *Mater. Res. Bull.* **84** 15
- [9] Tang P, Tong Y, Chen H, Cao F and Pan G 2013 *Curr. Appl. Phys.* **13** 340
- [10] Li S, Zhao Y, Wang C, Li D and Gao K 2016 *Mater. Lett.* **170** 122

- [11] Afifah N and Saleh R 2016 *J. Phys. Conf. Ser.* **710** 012030
- [12] Afifah N and Saleh R 2016 *Mater. Sci. Forum* **864** 99
- [13] Derikvandi H and Nezamzadeh-Ejhi A 2017 *J. Hazard. Mater.* **321** 629
- [14] Afifah N, Djaja N F and Saleh R 2015 *Mater. Sci. Forum* **827** 19
- [15] Phokha S, Pinitsoontorn S, Maensiri S and Rujirawat S 2014 *J. Sol-Gel Sci. Technol.* **71** 333
- [16] Abazari R and Sanati S 2013 *Superlattice. Microst.* **64** 148
- [17] Kaur J and Singhal S 2014 *Ceram. Int.* **40** 741
- [18] Yang Y, Que W, Zhang X, Xing Y, Yin X and Du Y 2016 *J. Hazard. Mater.* **317** 430
- [19] Nezamzadeh-Ejhi A and Ghanbari-Mobarakeh Z 2015 *J. Ind. Eng. Chem.* **21** 668
- [20] Saleh R and Djaja N F 2014 *Superlattice. Microst.* **74** 217
- [21] Cai A, Wang X, Qi Y and Ma Z 2017 *Appl. Surf. Sci.* **391** 484